Intensity Based Visualization of Pulmonary Biomarkers on Ultrashort Echo Time (UTE) MRI

Darren Hsu

Electrical Engineering and Computer Sciences
University of California, Berkeley

Technical Report No. UCB/EECS-2023-46
http://www2.eecs.berkeley.edu/Pubs/TechRpts/2023/EECS-2023-46.html

May 1, 2023

Intensity Based Visualization of Pulmonary Biomarkers on Ultrashort Echo Time (UTE) MRI

by

Darren Hsu

A thesis submitted in partial satisfaction of the

requirements for the degree of

Master of Science

in

Electrical Engineering and Computer Science

in the

Graduate Division

of the

University of California, Berkeley

Committee in charge:

Professor Michael Lustig, Chair
Professor Peder Larson

Spring 2022

Intensity Based Visualization of Pulmonary Biomarkers on Ultrashort Echo Time (UTE) MRI

by Darren Hsu

Research Project

Submitted to the Department of Electrical Engineering and Computer Sciences, University of California at Berkeley, in partial satisfaction of the requirements for the degree of **Master of Science, Plan II**.

Approval for the Report and Comprehensive Examination:

Committee:

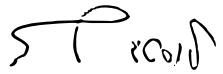

Professor Michael Lustig
Research Advisor

5/7/22

(Date)

* * * * * * *

Professor Peder Larson
Second Reader

(Date)

Intensity Based Visualization of Pulmonary Biomarkers on Ultrashort Echo Time (UTE) MRI

Abstract

Intensity Based Visualization of Pulmonary Biomarkers on Ultrashort Echo Time (UTE) MRI

by

Darren Hsu

Master of Science in Electrical Engineering and Computer Science

University of California, Berkeley

Professor Michael Lustig, Chair

Current non-invasive pulmonary function tests include spirometry and plethysmography, which assess lung volume, rates of flow, and gas exchange in both lungs. These tests can collectively measure aggregate respiratory metrics of both lungs, but not the right or left lung separately. This key drawback motivates a localized approach, through signal intensity based pulmonary function biomarkers. Recent advances in ultrashort echo time (UTE) MRI allows for robust imaging in pulmonary free-breathing exercises, without harmful ionizing radiation. Applying signal intensity based methods, biomarker metrics such as time to signal intensity peak (TTP) or full width at half maximum (FWHM) intensity are extracted from the image. The resulting visualizations depict localized respiratory function to help clinicians understand the rate and velocity at which lung tissue expands from full inspiration to full expiration.

Contents

List of Figures

Acknowledgments

Throughout my undergraduate and graduate studies, I have received immense support for my research goals. I would like to thank my Faculty Advisor, Professor Michael (Miki) Lustig, for his continuous advice and guidance. I would also like to thank Professor Peder Larson, for his invaluable insights throughout the project. Furthermore, a special thank you to Fei Tan, who provided me with all the necessary resources for me to succeed as a researcher. Finally, a special shout out to Ke Wang for his mentorship and being a constant cheerleader.

Chapter 1

Introduction

1.1 Background

Magnetic Resonance Imaging (MRI)

Magnetic resonance imaging (MRI) is a high-resolution medical imaging modality that allows clinicians to gain visibility inside the human body, without using harmful ionizing radiation. Its comparative advantage over ionizing imaging methods, such as chest X-rays and computed tomography (CT), is well recognized [1]. In pediatric patients or pregnant women, where radiation exposure may be harmful, MRI based methods stand to compete as a powerful alternative imaging technique.

Ultrashort Echo Time (UTE) MRI

Historically, low proton density, fast signal decay, and respiratory movement in the lung made images susceptible to artifacts [2]. As a result, it was challenging to generate a high signal-to-noise ratio (SNR) images of the lung. To overcome these challenges, 1H (proton) MRI is used to exploit the resonant high-frequency signal of protons in lung tissues and liquids. Recent advances in 1H (proton) ultrashort echo time (UTE) MRI allow for motion robust imaging in pulmonary free breathing images [3]. With these advances in pulmonary MRI, it is now possible to generate high SNR images of the lung [4].

1.2 Motivation

Current non-invasive pulmonary function tests include spirometry and plethysmography, which assess lung volume, rates of flow, and gas exchange in both lungs [5]. These tests can collectively measure aggregate respiratory metrics of both lungs, but not the right or left lung separately [6]. This key drawback motivates a localized approach, through signal intensity based pulmonary function biomarkers. In past papers, signal intensity biomarkers

have been shown to measure lung function, lung movement, and respiratory function [7, 8, 9]. Using the time to peak (TTP) and full width at half max (FWHM) biomarkers, we will show that signal intensity based biomarkers are a viable alternative to spirometry and plethysmography tests. The TTP biomarker was selected for its property of characterizing the peak of respiratory motion. The FWHM biomarker was chosen because it provides insight into the speed of respiratory motion.

1.3 Related Work

There has been considerable work done in developing pulmonary biomarkers, so we will discuss two relevant methodologies.

Pulmonary Ventilation Analysis

In a recent study, pulmonary ventilation analysis was performed on UTE free breathing lung MRI for the first time [10]. The paper sought to quantify regional ventilation through a localized approach. The resulting ventilation maps showed that they were reproducible and were able to show lung abnormalities in patients with Bronchiolitis Obliterans (an inflammatory obstruction of the lung's tiniest airways).

Using UTE 1H (proton) MRI, the authors were able to leverage structural and functional information of the lung. Furthermore, respiratory motion-resolved 3D imaging enables the separation of several respiratory states between expiration and inspiration. After data acquisition, each respiratory state was registered to the end expiratory state with three different methods.

1. Cyclic Registration: B-spline 3D+t cyclic registration utilizes the sinusoidal characteristic of breathing patterns in the human respiratory system.

2. Multi B-spline Registration: Multi B-spline registration is a deformable registration method that accounts for sliding motion of the lung across the chest wall.

3. Symmetric image normalization (SyN): SyN registration with the mutual information metric minimizes the effect of intensity changes during respiratory motion.

By analyzing the lung tissue deformation variation across the expiratory and inspiratory phases, a motion field for the respiratory movement was generated. To create the visualizations, the Jacobian determinant was applied to quantify the ratio of volume at the respiratory state to the end expiration state.

The key point was that regional ventilation biomarker methods using the Jacobian determinant of the motion field are feasible and reproducible in healthy volunteers. All three registration methods (cyclic registration, multi-b-spline, and SyN) showed similar reproducibility in the pulmonary ventilation analysis. In future studies, the authors seek to conduct more

MRI scans on patients with cystic fibrosis and other lung diseases to assist their diagnosis with precise treatments.

Phase-Resolved Functional Lung (PREFUL) MRI Biomarkers

In a feasibility study, dynamic perfusion and ventilation biomarkers were extracted from 1H (proton) MRI [7]. The authors demonstrated the practical implementation of phase-resolved functional lung imaging to gain quantitative information regarding regional lung perfusion and ventilation, without the need for ultrafast imaging.

Through their study, healthy volunteers and patients with cystic fibrosis were imaged. Afterward, the subject time series images were registered to a fixed image in the intermediate lung position. To increase the signal-to-noise ratio, edge-preserving guided image filtering was applied. To model the human respiratory motion, a sinusoidal curve fitting model was fit to the signal intensity values. The perfusion-weighted maps were then generated with the TTP PREFUL biomarkers.

The resulting PREFUL biomarkers depicted a pattern of below average hypoventilation and decreased perfusion for the cystic fibrosis patient when compared to the healthy volunteer. The PREFUL biomarkers had visual agreement with clinical CT scans. This study depicts the feasibility of obtaining quantitative information regarding regional lung perfusion and ventilation by applying phase-resolved functional lung imaging. By removing the need for ultrafast imaging, clinicians will benefit in future clinical translation studies.

Chapter 2

Methods

2.1 Methods Overview

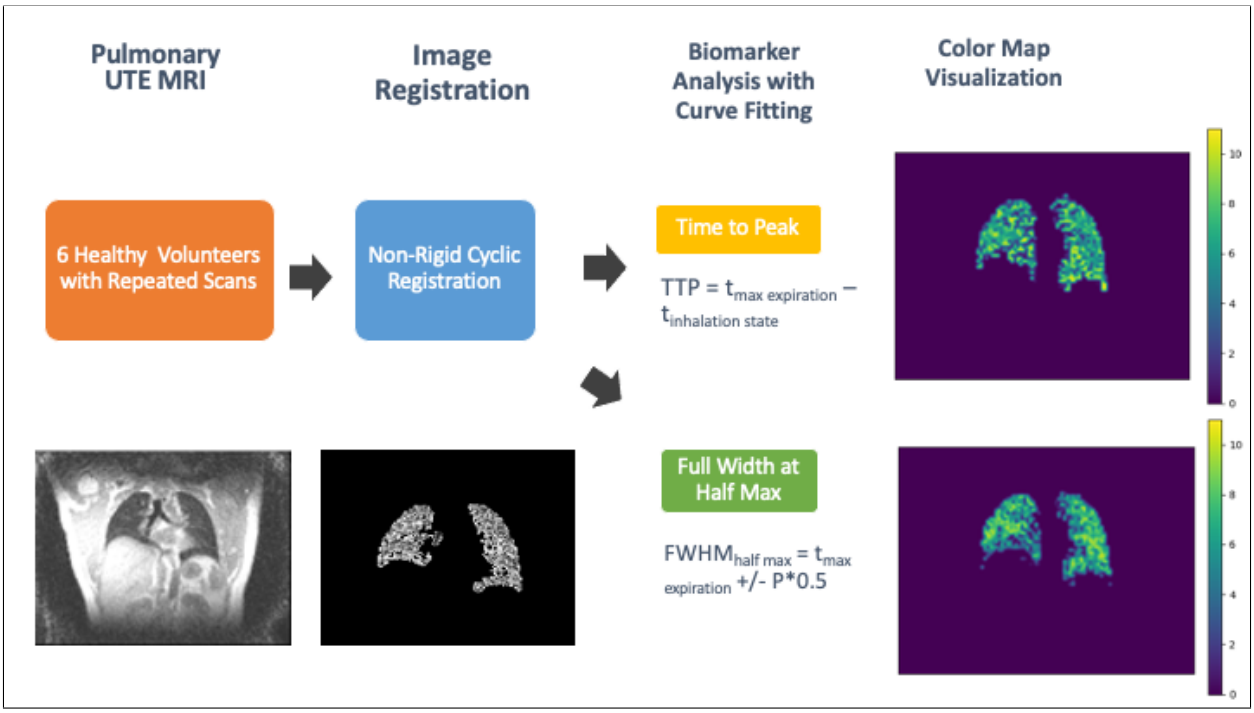

Figure 2.1: Overview of the biomarker visualization pipeline.

Figure 2.1 depicts the full pulmonary biomarker pipeline for one representative healthy volunteer. In summary, the application of the time to peak and full width at half max biomarker methods presented are as follows:

1. Free breathing pulmonary ultra short echo time (UTE) MRI scans were acquired on six healthy volunteers with repeated scans.
2. Twelve phases were reconstructed to segment respiratory motion using self-navigation phase-resolved reconstruction.
3. A non-rigid cyclic registration algorithm registered the respiratory states to the end expiratory state.
4. Using the ANTsPyNet package, a lung mask was generated to segment the 3D pulmonary image from human tissue.
5. Application of denoising methods included voxel generation and strided convolutions with padding.
6. With a voxel based approach, a 3rd and 4th degree polynomial curve fitting model was applied in the respiratory phase direction.
7. Time to peak (TTP) and full width at half max (FWHM) biomarkers were generated from the polynomial curve fitting models.

2.2 Subjects

Six healthy volunteers, aged 23-30, were recruited to participate in the study. The MRI scans were performed during free breathing. This study was approved by the University of California, San Francisco Institutional Review Board ethics committee, and written informed consent was obtained from all participants.

2.3 Imaging Procedure

Pulmonary MR images were acquired on a 3T MR750 clinical scanner (GE Healthcare, Waukesha, WI) with an 8-channel cardiac phased-array coil using 3D radial UTE sequences [3]. A golden angle ordering with variable-density 3D radial UTE sequence was used during the free-breathing scan [10]. The parameters were: flip angle=4°, FOV=40cm, TE/TR=0.1 / 2.4ms, BW=+/-125kHz, number of spokes=200,000, resolution=2.5mm isotropic [11]. Subjects were scanned twice on the same day for reproducibility.

2.4 Registration and Denoising

The raw data was segmented into twelve phases according to the respiratory motion and reconstructed using self-navigating, phase-resolved reconstruction [12]. The respiratory states were registered to the end expiratory states using the non-rigid cyclic registration algorithm [13]. After registration, the ANTsPyNet package [14] created a lung mask with a morphology closing diameter of 3 voxels. The lung mask was then utilized to extract the 3D pulmonary image from the rest of the tissue. Since signal intensity values of pulmonary tissue vary with expansion and contraction between phases, we analyze signal intensities through a voxel-based approach. Lung tissue has higher proton density providing higher signal intensity during contraction and presenting lower signal in expansion. A 2x2x2 voxel size was chosen for strided image convolutions to reduce the noise in the image. Voxel padding was also added for the strided convolutions.

2.5 Respiratory Cycle Reconstruction

Intensity values were smoothed in the respiratory phase direction by using a third and fourth degree polynomial curve fitting model. Afterward, a polynomial curve fitting model was generated for each voxel of the pulmonary lung image, along the respiratory dimension. As a result of the polynomial curve fitting process, the 4D images were transformed into 3D images since each voxel now contains a unique biomarker metric. Please reference section 2.6 for biomarker calculations. A polynomial curve fitting model was chosen due to the robustness of the additional degrees of freedom, compared to a sinusoidal or Gaussian curve fitting model.

The least squares polynomial fit was used to minimize the variance of the unbiased estimators of the coefficients. In the polynomial curve fitting model, we are solving for the unknown β parameter values shown below:

$$y = \beta_0 + \beta_1 x + \beta_2 x^2 + \beta_3 x^3 + \cdots + \beta_n x^m \tag{2.1}$$

Expressing the polynomial curve fitting model in matrix form, we reach the following below. Equation 2.2 contains the Vandermonde matrix $\mathbf{X}$, output vector $\vec{y}$, and unknown parameter β values. Since the TTP and FWHM biomarkers in section 2.6 were fit to third or fourth degree polynomials, m=3 or m=4. Each i-th row of the Vandermonde matrix $\mathbf{X}$ will be a unique data point with its corresponding i-th output y value. Since respiratory motion is segmented into twelve bins, n=12 for the twelve data points in the respiratory dimension.

$$\begin{bmatrix} y_1 \\ y_2 \\ y_3 \\ \vdots \\ y_n \end{bmatrix} = \begin{bmatrix} 1 & x_0 & x_0^2 & \cdots & x_0^m \\ 1 & x_1 & x_1^2 & \cdots & x_1^m \\ 1 & x_2 & x_2^2 & \cdots & x_2^m \\ \vdots & \vdots & \vdots & \ddots & \vdots \\ 1 & x_n & x_n^2 & \cdots & x_n^m \end{bmatrix} \begin{bmatrix} \beta_0 \\ \beta_1 \\ \beta_2 \\ \vdots \\ \beta_m \end{bmatrix} \tag{2.2}$$

Writing the matrices in vector matrix form, we arrive at:

$$\vec{y} = \mathbf{X}\vec{\beta} \tag{2.3}$$

Applying ordinary least squares estimation, the β values are estimated with:

$$\widehat{\vec{\beta}} = (\mathbf{X}^{\mathsf{T}}\mathbf{X})^{-1}\,\mathbf{X}^{\mathsf{T}}\vec{y}, \tag{2.4}$$

2.6 Pulmonary Biomarker Analysis

In this paper, we propose two different biomarkers, the time to peak (TTP) and the full width at half max (FWHM).

Time to Peak (TTP)

For calculating the TTP biomarker, the vertical position of the maximum signal intensity value correlated with the expiratory state is calculated. The difference between the maximum expiratory state and the inspiratory state constitutes TTP, where t is time in phase state.

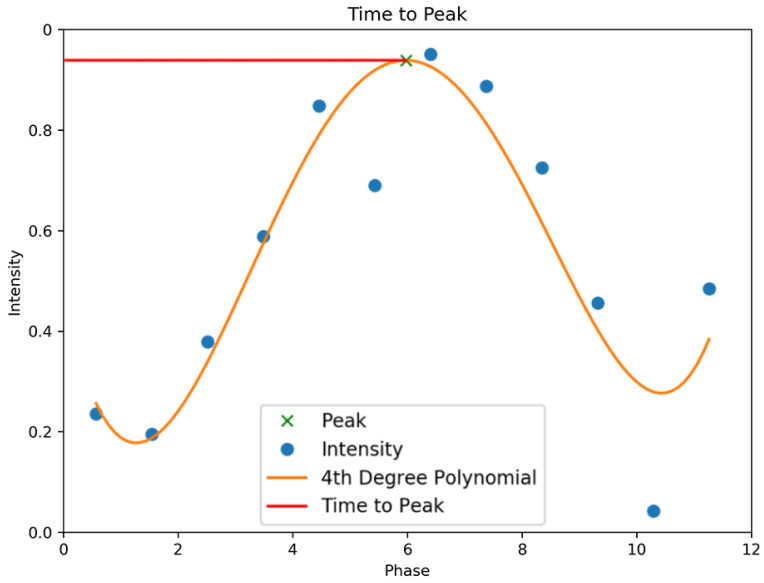

Figure 2.2: The Time to Peak Biomarker of a representative voxel sample across the phase dimension of respiratory motion.

$$Time\ to\ Peak\ (TTP) = t_{max\ \ expiration} - t_{inhalation\ \ state} \tag{2.5}$$

Full Width at Half Max (FWHM)

For the FWHM biomarker, the distance between two points where the function reaches half of its maximum value is calculated. Taking the difference between these two points yields the biomarker FWHM. The variable P is the peak's prominence and is calculated at the maximum expiration state, where the intensity value is the highest.

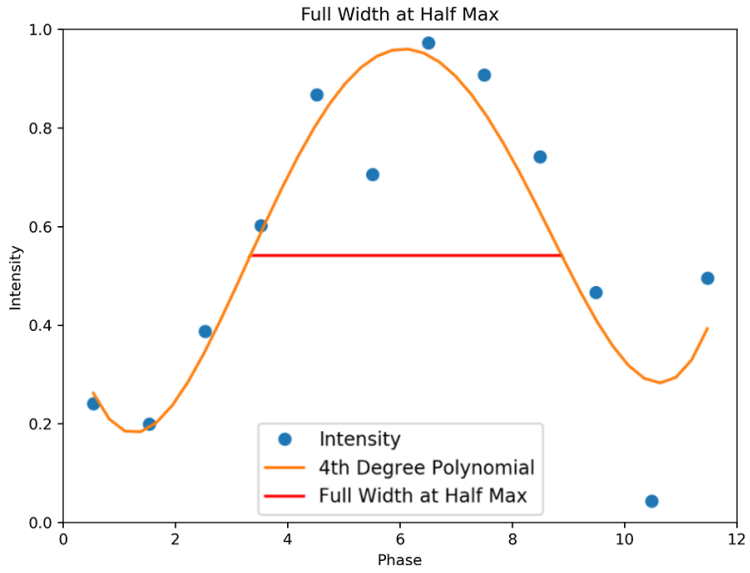

Figure 2.3: The Full Width at Half Max Biomarker of a representative voxel sample across the phase dimension of respiratory motion.

$$Full\ Width\ at\ Half\ Max\ (FWHM) = h_{half\ max,right} - h_{half\ max,left} \tag{2.6}$$

$$h_{half\ max} = t_{max\ expiration} \pm P * 0.5 \tag{2.7}$$

2.7 Reproducibility

For the reproducibility metric, the root mean squared (RMS) and logarithmic within-subject coefficient of variation (CV) were calculated [15]. X_1 and X_2 are pulmonary function biomarkers from repeated scans of the same subject. X_1 and X_2 were calculated by averaging all TTP or FWHM biomarker voxels, with their respective 3rd or 4th degree curve fitting methods.

For the RMS coefficient of variance, the mean of the two scans were first calculated in equation 2.9. Applying the root mean squared, we arrive at the equation below:

$$RMS\ Coefficient\ of\ Variance\ (\%) = \sqrt{\frac{\sum \left(\frac{X_1 - X_2}{Mean}\right)^2}{2n}} \times 100 \tag{2.8}$$

$$Mean = \frac{\sum (X_1 + X_2)}{2n} \tag{2.9}$$

For the logarithm coefficient of variance, exponentiating the log of the X_1 and X_2 scans arrives at this equation below:

$$Log\ Coefficient\ of\ Variance\ (\%) = (\exp \sqrt{\frac{\sum (\log X_1 - \log X_2)^2}{2n}} - 1) \times 100 \tag{2.10}$$

Chapter 3

Results

3.1 TTP and FWHM Biomarkers

Applying the biomarker reconstruction pipeline, Figure 3.1 and Figure 3.2 depict the coronal plane and sagittal plane, respectively, of the TTP and FWHM pulmonary biomarkers.

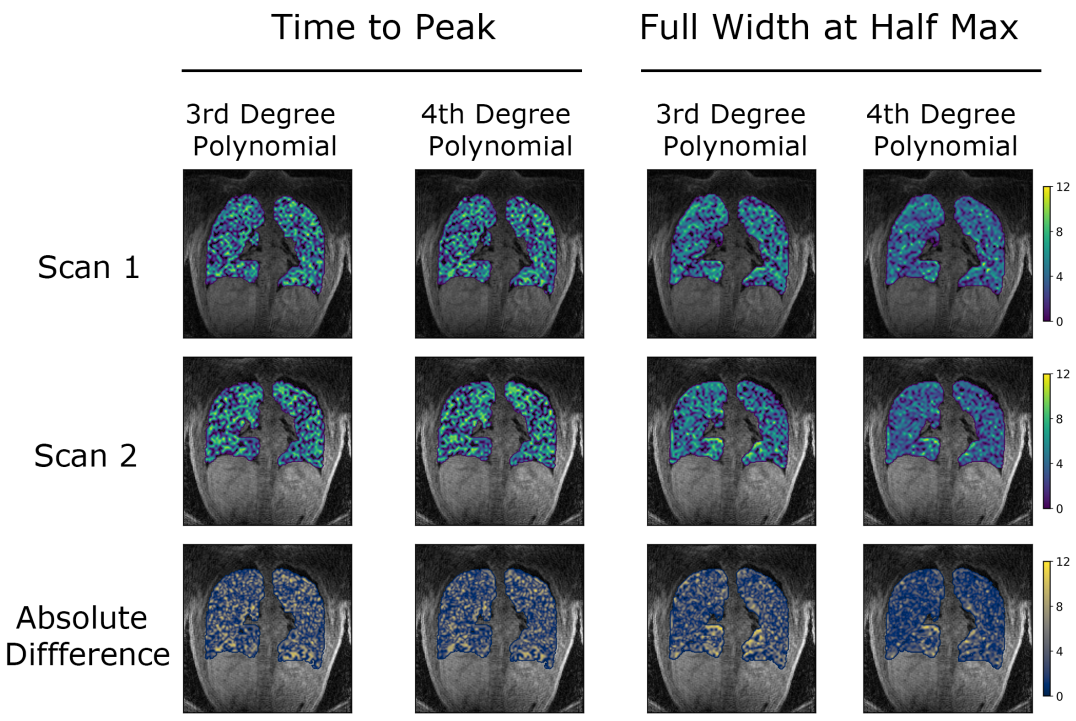

Figure 3.1: Coronal Plane of the Time to Peak and Full Width at Half Max Biomarkers

Each biomarker was overlaid on a registered phase-resolved lung MR image for one representative volunteer. For reproducibility, each subject was scanned twice in the same day with the same imaging procedures and MRI sequences. As shown, all four biomarkers exhibit homogeneous ventilation on the colormap visualization. The absolute difference of the biomarkers also exhibit a uniform distribution of the voxel biomarker intensity values.

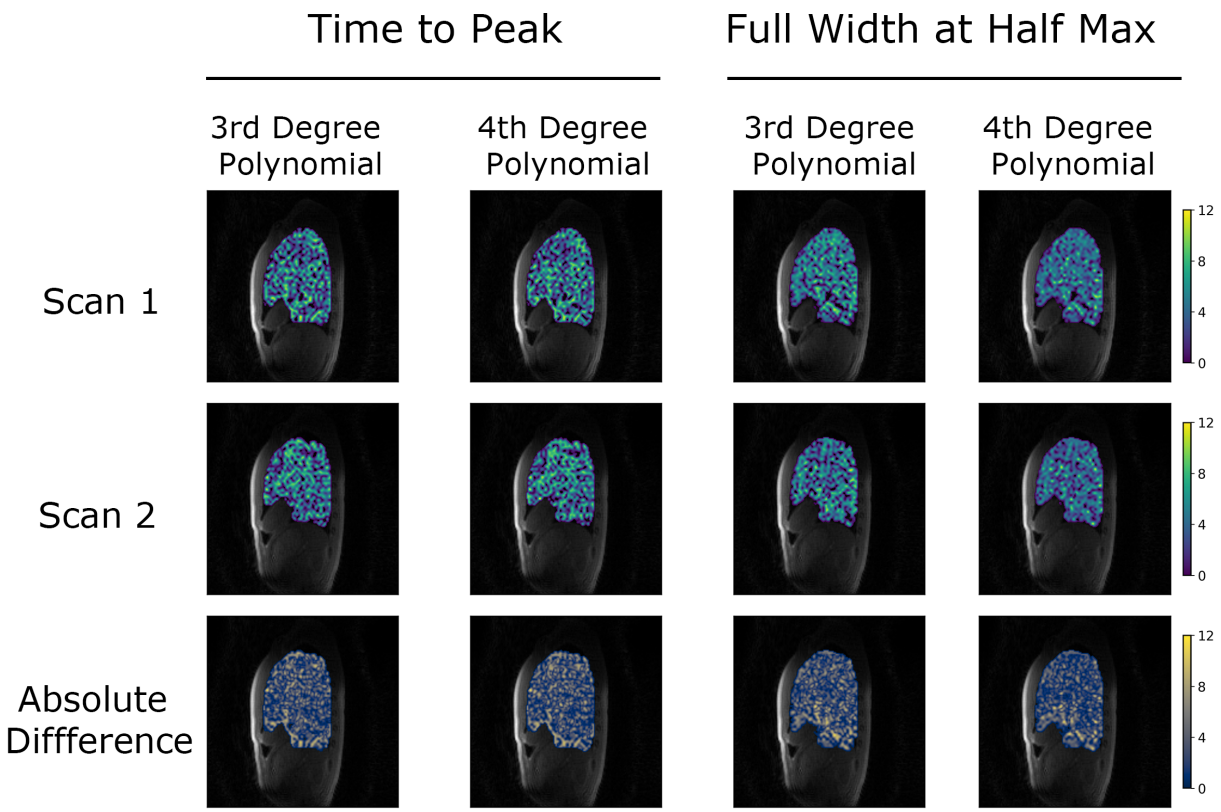

Figure 3.2: Sagittal Plane of the Time to Peak and Full Width at Half Max Biomarkers

3.2 Reproducibility

Coefficient of Variation from Repeated Scans

Figure 3.3 shows the RMS and logarithm within-subject coefficient of variation boxplot and the data table. The boxplot indicates that the TTP third degree polynomial has a lower median than the fourth degree polynomial but with a higher variance. For FWHM, both polynomial curve fitting methods have similar medians but the 4th degree polynomial has lower variance, which suggests that the 4th degree polynomial curve fitting methods are more reproducible.

Within-Subject Coefficient of Variance (CV)

		TTP 3rd Degree Polynomial	TTP 4th Degree Polynomial	FWHM 3rd Degree Polynomial	FWHM 4th Degree Polynomial
Subject 1	Log CV	6.82%	4.78%	8.31%	7.23%
	RMS CV	6.59%	4.67%	7.97%	6.98%
Subject 2	Log CV	3.25%	5.61%	6.07%	5.10%
	RMS CV	3.19%	5.46%	5.88%	4.97%
Subject 3	Log CV	1.14%	6.85%	21.52%	18.05%
	RMS CV	1.13%	6.62%	19.37%	16.52%
Subject 4	Log CV	3.30%	5.69%	7.79%	8.67%
	RMS CV	3.25%	5.53%	7.49%	8.31%
Subject 5	Log CV	7.50%	5.92%	16.79%	12.93%
	RMS CV	7.23%	5.75%	15.46%	12.13%
Subject 6	Log CV	3.72%	4.40%	3.30%	3.36%
	RMS CV	3.65%	4.30%	3.25%	3.30%

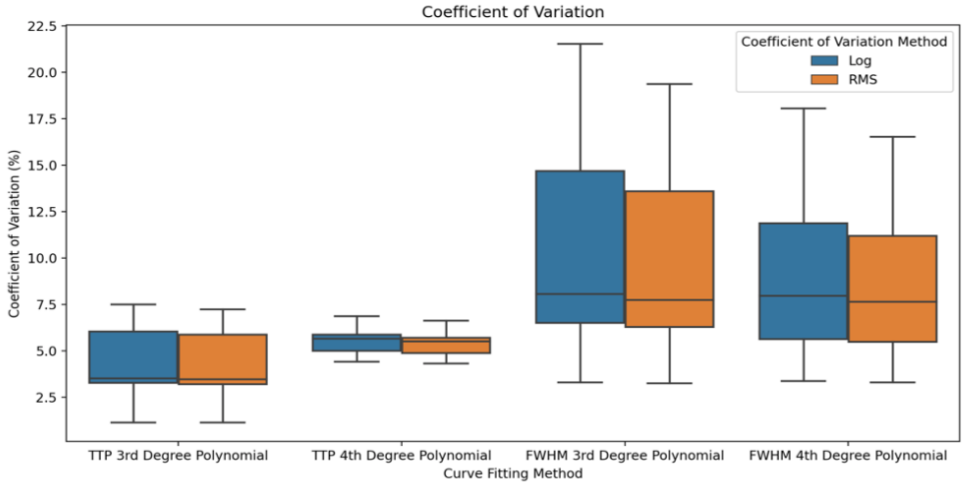

Figure 3.3: Within subject coefficient of variation (CV) table and the corresponding box plot. For the reproducibility metric, the root mean squared (RMS) and logarithmic within-subject coefficient of variation were calculated. A CV value closer to zero indicates smaller differences between the two repeated scans and thus the pulmonary function biomarkers are more reproducible.

Distribution of Biomarker Intensities

Figure 3.4 shows the split violin plot of repeated scans of the same subject, using the four biomarker methods. The median of the two FWHM biomarkers ranged from 6-7, with a normal distribution of values. The median of the two TTP biomarkers ranged from 7-8, with a skewed distribution of values.

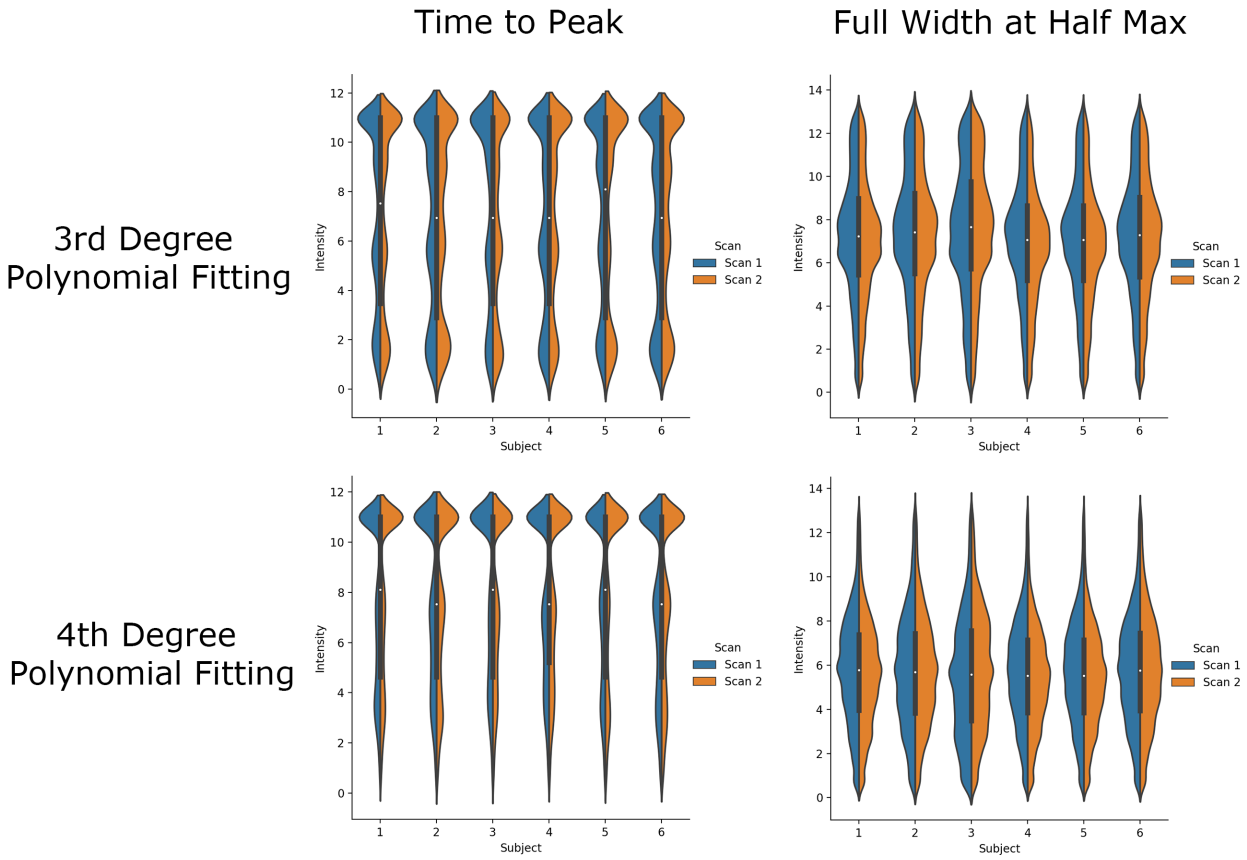

Figure 3.4: A split violin plot of each pulmonary function biomarker is created. The x-axis shows the six subjects recruited for the study. The y-axis is the value of each biomarker metric. The shaded area of each half of the violin plot represents the frequency of each respective biomarker metric.

Chapter 4

Discussion

The main findings of this study are as follows:

1. The TTP biomarker likely reflects the rate at which lung tissue expands from the full inspiration to the full expiration phase.
2. The FWHM biomarker depicts the velocity of the tissue expansion from inspiration to expiration, as it describes the width of the signal intensity peak.
3. Both the TTP and FWHM biomarkers are reproducible based on the RMS within subject CV and Logarithm within subject CV.

4.1 Time to Peak (TTP)

For the reconstructed images, phase one corresponds to inspiration while phase seven corresponds to expiration. For the TTP biomarker, a value of seven is to be expected as the seventh phase corresponds to exhalation, representing the highest signal intensity value. In Figure 3.4 of the TTP violin plots, the distribution of values is clustered at the end of the distribution. This is due to the high intensity white noise in the inspiration phase. This phenomenon can be fixed with precise binning of phases and inspiration-expiration matching.

4.2 Full Width Half Max (FWHM)

For the FWHM biomarker, a value of six is expected, since it will capture the phases before and after full exhalation. In the coronal plane and sagittal plane figures, the between-scan difference shows uniform variation. For the Figure 3.3 boxplots, we see that the variance of FWHM is greater than the TTP biomarkers. This can be explained by noise or artifacts in the scans since subjects 3 and 5 saw elevated CV.

Chapter 5

Conclusion

This study underscores the feasibility of utilizing intensity based biomarkers to provide quantitative insight into regional pulmonary function. The TTP biomarker likely reflects the rate at which lung tissue expands from the full inspiration to the full expiration phase. The FWHM biomarker depicts the velocity of the tissue expansion from inspiration to expiration, as it describes the width of the signal intensity peak.

In essence, all four biomarkers showed similar reproducibility in healthy volunteers. The 3rd degree and 4th degree TTP polynomial fits are equally reproducible while the 4th degree FWHM is more reproducible than the 3rd degree FWHM.

The ultimate goal is to use pulmonary respiratory biomarkers on all human subjects in clinical studies. We demonstrated significant improvement in providing quantitative insight into respiratory motion, and we hope that this system can be used to improve future clinical research.

5.1 Future Work

In this project, we have demonstrated the efficacy of using the TTP and FWHM biomarkers on healthy human volunteers. Further studies of patients with cystic fibrosis or chronic obstructive pulmonary disease (COPD) can assess the efficacy of these biomarker results. Furthermore, we seek to apply these pulmonary biomarkers to pediatric patients since they would benefit from the non-ionizing radiation of MRI.

Additional work in developing a robust noise filtering model for post-processing pulmonary images would be extremely beneficial. Due to the nature of intensity based visualization of biomarkers, the biomarkers themselves are sensitive to noise. In this paper, we utilized voxel based analysis and strided image convolutions to increase the signal-to-noise ratio. To increase the SNR ratio even further, more aggressive filtering methods would need to be applied.

Bibliography

[1] Hersh Chandarana et al. "Emerging role of MRI in radiation therapy". In: *Journal of Magnetic Resonance Imaging* 48.6 (2018), pp. 1468–1478.

[2] M. Puderbach et al. "MR imaging of the chest: A practical approach at 1.5T". In: *European Journal of Radiology* 64.3 (2007). Pulmonary Functional Imaging, pp. 345–355. ISSN: 0720-048X. DOI: https://doi.org/10.1016/j.ejrad.2007.08.009. URL: https://www.sciencedirect.com/science/article/pii/S0720048X07003889.

[3] Kevin M Johnson et al. "Optimized 3D ultrashort echo time pulmonary MRI". In: *Magnetic resonance in medicine* 70.5 (2013), pp. 1241–1250.

[4] J Biederer et al. "MRI of the lung (2/3). Why... when... how?" In: *Insights into imaging* 3.4 (2012), pp. 355–371.

[5] C.P. Criée et al. "Body plethysmography – Its principles and clinical use". In: *Respiratory Medicine* 105.7 (2011), pp. 959–971. ISSN: 0954-6111. DOI: https://doi.org/10.1016/j.rmed.2011.02.006. URL: https://www.sciencedirect.com/science/article/pii/S0954611111000552.

[6] Heather M. Young, Rachel L. Eddy, and Grace Parraga. "MRI and CT lung biomarkers: Towards an in vivo understanding of lung biomechanics". In: *Clinical Biomechanics* 66 (2019). SI: Clinical Relevance of Respiratory Mechanics and Flows, pp. 107–122. ISSN: 0268-0033. DOI: https://doi.org/10.1016/j.clinbiomech.2017.09.016. URL: https://www.sciencedirect.com/science/article/pii/S0268003317302103.

[7] Andreas Voskrebenzev et al. "Feasibility of quantitative regional ventilation and perfusion mapping with phase-resolved functional lung (PREFUL) MRI in healthy volunteers and COPD, CTEPH, and CF patients". In: *Magnetic resonance in medicine* 79.4 (2018), pp. 2306–2314.

[8] Petros Martirosian et al. "Quantitative lung perfusion mapping at 0.2 T using FAIR True-FISP MRI". In: *Magnetic Resonance in Medicine: An Official Journal of the International Society for Magnetic Resonance in Medicine* 55.5 (2006), pp. 1065–1074.

[9] Ilyes Benlala et al. "Quantification of MRI T2 Interstitial Lung Disease Signal-Intensity Volume in Idiopathic Pulmonary Fibrosis: A Pilot Study". In: *Journal of Magnetic Resonance Imaging* 53.5 (2021), pp. 1500–1507.

[10] Fei Tan, Xucheng Zhu, and Peder EZ Larson. "Pulmonary Ventilation Analysis Using 1H Ultra-short Echo Time (UTE) Lung MRI: A Reproducibility Study". In: *Proc. International Society for Magnetic Resonance* (2021).

[11] Darren Hsu et al. "Intensity Based Visualization of Pulmonary Function Using Time to Peak and Full Width at Half Max Biomarkers on Ultrashort Echo Time (UTE) MRI". In: *Proc. International Society for Magnetic Resonance* (2021).

[12] Fei Tan, Xucheng Zhu, and Peder EZ Larson. "Dynamic 3D Ventilation Maps with Phase-Resolved Ultrashort Echo Time (UTE) MRI". In: *Proc. International Society for Magnetic Resonance* (2020).

[13] Coert T Metz et al. "Nonrigid registration of dynamic medical imaging data using nD+ t B-splines and a groupwise optimization approach". In: *Medical image analysis* 15.2 (2011), pp. 238–249.

[14] Nicholas J Tustison et al. "ANTsX: A dynamic ecosystem for quantitative biological and medical imaging". In: *medRxiv* (2020), pp. 2020–10.

[15] J Martin Bland and Douglas G Altman. "Measurement error proportional to the mean." In: *BMJ: British Medical Journal* 313.7049 (1996), p. 106.